

The thermo-mechanical performance of glass-fibre reinforced Polyamide 66 during glycol-water hydrolysis conditioning.

J. L. Thomason, J.Z. Ali and J. Anderson

University of Strathclyde, Department of Mechanical Engineering, 75 Montrose Street, Glasgow G1 1XJ, United Kingdom.

Abstract

Injection moulded glass-fibre reinforced polyamide 66 composites based on two glass fibre products with different sizing formulations and unreinforced polymer samples have been characterised by dynamic mechanical analysis and unnotched Charpy impact testing both dry as moulded and during conditioning in a glycol-water mixture at 70°C for a range of times up to 400 hours. Simultaneously weight and dimension changes of these materials have been recorded. The results reveal that hydrothermal ageing in glycol-water mixtures causes significant changes in the thermo-mechanical performance of these materials. It is shown that mechanical performance obtained after conditioning at different temperatures can be superimposed when considered as a function of the level of fluid absorbed by the composite polymer matrix.

Introduction

Glass fibre reinforced polyamides, such as polyamide 6 and 66, are excellent composite materials in terms of their high levels of mechanical performance and temperature resistance. However, the mechanical properties of polyamide based composites decrease markedly upon absorption of water and other polar fluids. The mechanical performance of these composites in a hydrothermal environment results from a combination of the fibre and matrix properties and the ability to transfer stresses across the fibre-matrix interface. Variables such as the fibre content, diameter, orientation and the interfacial strength are of prime importance to the final balance of properties exhibited by injection moulded thermoplastic composites [1-5]. Short fibre reinforced thermoplastics have been used in the automotive industry for many years and there has recently been a strong growth in the use of polyamide based materials in under-the-hood applications [6]. These applications place stringent requirements on such materials in terms of dimensional stability and mechanical, temperature and chemical resistance. There has been a rapid increase in the number of moulded composites exposed to engine coolant at high temperatures [7-10] and this has led to a need for an improvement in our understanding of the performance of glass-reinforced-polyamide under such conditions.

Typical testing for these applications involves measurement of mechanical properties before and after conditioning of the test material in model coolant fluids for a fixed time, up to 3000 hours, at temperatures in the 100-150°C range [10]. It is not always easy to obtain a good understanding of the structure-performance relationships of a material from such snapshots of performance taken at a single condition. However, it has been known for sometime within the industry that the chemical nature of the glass fibre sizing can have a strong influence on the retention of some mechanical properties of composites exposed to such hydrothermal conditioning. It is also well known that

polyamide materials absorb relatively high levels of moisture when exposed to hydrothermal conditioning in water and that this can cause significant dimensional changes [11-17]. Despite this, and the fact that such hydrothermal testing has become commonplace for under-the-hood applications, there has been little systematic investigation of dimensional change of glass-fibre reinforced polyamide composites during such conditioning in coolant fluid. Thomason [17] has recently reviewed the mechanical performance and dimensional changes observed in glass fibre reinforced polyamide 66 during conditioning in coolant fluid at 120°C and 150°C. A rapid reduction was observed in both the modulus and strength of these composites and the matrix polymer in the initial stage of conditioning. However, unnotched impact was seen to initially increase significantly. Due to the rapid rate of fluid absorption and dimensional change at these high temperatures it was not possible to examine these effects in detail. The weight and dimensional changes in these materials during condition at lower temperatures (70°C) has recently been reported [18]. This paper presents the results of a study of the changes in the thermo-mechanical performance of injection moulded glass reinforced polyamide 66 composites during hydrothermal conditioning in model coolant fluid. Composites have been prepared using two chopped glass products where one contains a sizing system which has been optimised to improve the performance of composites subjected to hydrothermal treatments. To enable study of the initial stages of the process the conditioning temperature has been limited to 70°C for a range of conditioning times up to 400 hours. Data on the changes in the thermal and mechanical performance of these composites are presented and discussed in this paper.

Experimental

The injection moulded polymer and composite bars for this study were supplied by the 3B fibreglass company. The polyamide 66 (PA66) used was DuPont Zytel 101. Composite samples with 30% weight fibre content were produced using this polymer and two chopped Advantex™ E-glass products. Advantex™ is a boron free E-glass formulation. These products were chopped to a length of 4 mm and the individual fibres had a nominal average diameter of 10 µm. Both samples were coated with sizings which are designed for polyamide reinforcement. DS1143 is a typical sizing designed to maximise the “dry as moulded” (DaM) performance of glass reinforced polyamides. The main ingredients of such sizings are typically aminosilane coupling agent and a commercial polyurethane dispersion [19,20]. DS1110 sizing contains extra components which enhance the retention of composite mechanical properties in elevated temperature hydrolytic environments [21-23]. Three series of samples were moulded, series A using DS1143 glass, series B using DS1110 glass, and series R containing only the PA66 resin. The glass and polymer were compounded on a twin screw extruder and injection moulded to produce end-gated rectangular bars of with nominal dimensions 80x10x4 mm.

The test bars for this study were received vacuum packed in a DaM state. On removal from the packaging all samples were weighed and their three dimensions recorded at room temperature prior to conditioning. A micrometer with an operating range between 0-50mm ± 0.005mm was used in order to measure the width and the thickness of the test samples. It is well known that the cross section of injection moulded samples may not be exactly rectangular and it was noted that the recorded dimension varied slightly dependent on where the measurement was taken. To ensure consistency measurements were therefore taken at the exact centre of each sample, as per ISO 179. The sample bars

length exceeded the range of the micrometer and so the length of the test samples was measured using a Vernier calliper with an accuracy of ± 0.01 mm was used. A digital balance with an operating range between 0-20 g ± 0.0001 g was used to measure sample weights. Each data point presented is the average of measurements on seven individual samples. Since these samples were subsequently used for impact testing this means that each data point for each conditioning time was obtained on a different set of seven samples. Hydrolysis conditioning took place in a temperature controlled bath with samples fully immersed in a 50:50 mixture of glycol and water (GW) at 70°C. Samples were stacked vertically and individually in a specially constructed rack such that the fluid had access to all surfaces of each sample. Conditioning times were chosen in the range 0-400 hrs. On removal from the conditioning container surface fluid was removed from the samples with tissue and then they were again weighed and their dimensions recorded. These samples were then equilibrated at room temperature in a GW mixture for 24 hours after which they were again weighed and measured and then transferred immediately to the impact tester. Unnotched Charpy impact properties were measured on seven specimens in accordance with the procedures in ISO179-1 using a Tinius Olsen model IT503 Impact Tester set up with a 6.35J pendulum capacity. DMA measurements were made using a Polymer Laboratories Dynamic Mechanical Thermal Analyser MKIII, at a frequency of 1 Hz, a strain of $\times 4$, scanning rate of 4°C per minute and the samples were clamped with a torque of 40 Nm. Knife edged clamping was employed, using a frame which gave a sample length of 12 mm. Bending modulus and $\tan\delta$ were studied through a temperature range of -100°C to 150°C .

Results and Discussion

Moisture absorption related processes in polymers and composites are normally analysed against the square root of exposure time to enable the use of standard diffusion models [12-17,24] and this procedure has been followed in the figures which are presented here. Error bars in these figures represent the 95% confidence interval on the average value. Figure 1 shows such a plot of percentage increase in sample weight of the injection moulded impact bars for composites A and B and the resin only sample after hydrolysis at 70°C and prior to the 24 hour cooling and equilibration step in the experimental procedure. The data appears to show the main aspects typical of Fickian diffusion with a rapid initial uptake of liquid followed by a slow approach to an equilibrium absorption level. However, it is interesting to note that there does not appear to be a clear initial linear dependence of the weight increase as might be expected from a simple 1-D Fickian diffusion analysis [18,24]. It seems reasonable to assume that the glass fibres do not account for any of the weight increase seen during the hydrolysis treatment [12-18] and that the weight increase observed with the composites is solely due to weight changes of the polymer matrix. By dividing the composite weight increase by the average matrix content it is possible to examine the composite matrix weight change during these experiments. This data is also shown in Figure 1. It can be seen that at short conditioning times there is little significant difference in the level of fluid absorption between the composite matrices and the polymer sample. However at longer times (>24 hours) there is deviation from this trend and the composite matrices absorb significantly less fluid compared to the expectation based on the unreinforced polymer results. This has been previously observed to a greater degree in similar experiments carried out at higher temperatures and longer times [17]. Apparently the presence of the glass fibres reduces the ability of the polyamide matrix to absorb the

same level of fluid that is absorbed by the polymer in an unrestrained environment. It can also be seen in Figure 1 that there is no significant difference between the absorption results obtained with two composite systems A and B at this conditioning temperature.

In fluid absorption experiments in polymers, plate-shaped samples are generally preferred so that the fluid absorption is mainly determined by the uptake through the two broad faces of the plate. In this situation diffusion is approximated to occur in one direction only. Consequently, if fluid uptake is determined by classical Fickian diffusion, the fluid concentration can be approximated by the well known solution for diffusion in an infinite plate, which yields a linear increase in the weight increase of the sample with $t^{1/2}$ over the initial part of the experiment. However, when samples with different shapes are employed then corrections have to be made for edge effects where the sample weight is also increased by fluid uptake via the other available surfaces of a rectanguloid specimen. The necessary correction factors for such edge effects in samples of the dimensions used in this study have recently been reviewed [18]. If moisture uptake is determined by classical 1D Fickian diffusion, for diffusion in an infinite plate the moisture concentration then the mass of fluid adsorbed in time t , $M(t)$, as a fraction of the final equilibrium of M_e is given by [24]

$$\frac{M(t)}{M_e} = 1 - \frac{8}{\pi^2} \sum_{n=0}^{\infty} (2n+1)^{-2} \exp\left[-(2n+1)^2 \left(\frac{\pi^2 D_x t}{a^2}\right)\right] \quad (1)$$

Where D_x is the diffusivity in the x direction and a is the thickness in the x direction.

When $D_x t \ll 0.05a^2$ equation 1 can be reduced to

$$\frac{M(t)}{M_e} = \frac{4}{\pi^{1/2}} \left(\frac{D_x t}{a^2}\right)^{1/2} \quad (2)$$

And thus the diffusivity can be obtained from the initial linear portion of the absorption curve and the final equilibrium absorption level. In the case of fluid adsorption into a real 3-dimensional monolithic rectangular of dimensions a,b,c in the x,y,z directions where $D_c=D_x=D_y=D_z$ an edge correction factor f can [18,25] be introduced into equation 1 to give the effective diffusion coefficient

$$D_{eff} = f^2 D_c \quad (3)$$

$$f = 1 + 0.54 \frac{a}{b} + 0.54 \frac{a}{c} + 0.33 \frac{a^2}{bc} \quad (4)$$

The dimensions a,b,c correspond to the thickness, width and length of the injection moulded bars which results in a value of $f=1.212$. Using the above analysis and the initial slopes taken from the first data points in Figure 1 results in values of $D_{eff}= 12.0 \times 10^{-12} \text{ m}^2/\text{s}$ for the PA66 polymer and $10.4 \times 10^{-12} \text{ m}^2/\text{s}$ for the composites, which is in reasonable agreement with the values reported by Ishak and Berry [12]. However, given the apparent curvature of lines in Figure 1 it was also decided to fit the full curves using equation 1. The results of this exercise gave a better fit over a greater proportion of the curve is obtained using a value of $D_{eff}=5.3 \times 10^{-12} \text{ m}^2/\text{s}$ or $D_c=3.6 \times 10^{-12} \text{ m}^2/\text{s}$ for both polymer and composites. It was recently proposed [18] that these pseudo-Fickian effects could be explained by time dependent changes in D_c caused by changes in polymer crystallinity caused by the elevated temperature hydrolytic environment. This is shown in Figure 2 which shows the values of time dependent diffusion coefficient required to obtain a predicted weight gain which matches the experimentally observed values. In terms of later discussion, it should be noted in Figure 2 that the required value of time dependent diffusion coefficient reaches an approximately constant value after the polymer has absorbed 5-6% wt. of the GW fluid.

The results for the Charpy Unnotched impact strength are presented in Figure 3. It can be seen that glass B gives a significant higher DaM unnotched impact despite having the same fibre content. This difference is systematically maintained across the range of the hydrolysis experiments. In the early stages of the hydrolysis conditioning there is a small but significant drop in impact strength of both composites which reaches a minimum at approximately 12 hours conditioning. At longer times the unnotched impact starts to increase again and reaches a maximum value (+35-40% above the DaM value) at approximately 150 hours. At yet longer conditioning times the unnotched impact starts a slow decline but is still well above the DaM value at the maximum conditioning time of 400 hours. The polymer samples also exhibited a significant decrease in impact resistance which also reached a minimum after approximately 12 hours conditioning time. Further conditioning resulted in a rapid increase in the polymer impact strength, however it was observed that in the experiments where samples were conditioned longer than 25 hours not all of the samples could be broken in the impact test. This is reflected in the increase in the confidence limits observed on the last two points for the polymer samples in Figure 3. At conditioning times greater than 68 hours only 'no breaks' ($>160 \text{ kJ/m}^2$) were obtained with the polymer samples and so no further data points are shown in Figure 3. The unnotched impact performance of the PA66 polymer and composites is examined further in Figure 4 where the data are plotted as a function of the mass of fluid absorbed by the polymer or composite matrix. When presented in this manner it becomes clear that during the early stages of the GW conditioning the trends in impact performance of the composites correlates well with that of the polymer. Up to approximately 4% fluid uptake the impact performance decreases. When the level of absorbed fluid exceeds approximately 5-6% there is clear evidence of a change in impact performance with a sharp increase in both the polymer and composite impact strength. From a study of the viscoelastic behaviour of PA66

during condition in water at 60°C it has been suggested that a large scale change in the molecular structure of injection moulded PA66 takes place when the level of absorbed water exceeds 5% wt [26]. It is certainly an interesting correlation that the results on impact performance in this work also show an abrupt change in performance at approximately the same level of GW absorption.

The hydrolysis conditioning also resulted in significant changes in the dimensions of the polymer and composite samples [18]. The volume swelling of the polymer and composite samples after 70°C GW conditioning and equilibration at 23°C prior to impact testing is presented as a function of the polymer/matrix mass change in Figure 5. Both polymer and composite samples exhibit a linear relationship between the volumetric swelling and the mass of adsorbed fluid. However, there is clear evidence in the data in Figure 5 of a step increase in this relationship which occurs at approximately 6% fluid absorption in both the polymer and the composite matrix. Consequently, we have two independent measurements (Charpy impact and dimensional change) which appear to indicate some abrupt change taking place in the PA66 when the GW absorption level exceeds 5-6% wt. at 70°C. One possible explanation of this phenomenon is analogous to the Brill transition [27] which is well known in PA66. This is a broad transition of the crystal structure reported in dry PA66 between 160°C and 200°C but which has been observed to start as low as 80°C [28] and which is accompanied by changes in the thermal and mechanical properties [29]. This transition is observed crystallographically as a gradual transformation from the diffraction patterns with triclinic to pseudo-hexagonal symmetry, accompanied by a significant increase in volume [30] which is thought to contribute significantly to the relatively high level of thermal expansion observed in PA66 in this temperature range. The Brill transition has been considerably studied in dry PA66 and other polyamides as a function of

temperature, however, there is relatively little published on the effect of moisture. It has been reported [29] that the presence of moisture causes the Brill transition to occur at lower temperature. Changes in lamellar structure of PA6 and PA66 during hot GW absorption have been studied using small-angle neutron scattering [31]. It was reported that structural changes in polyamides are more severe with glycol than water alone and reported a significant reduction in the Brill transition temperature. In general it has been shown that the structure and crystallinity of polyamides can be radically altered by conditioning at elevated temperature and that these changes are accelerated in the presence of moisture [18]. Further direct investigation of changes to the crystal structure of PA66 undergoing hot GW conditioning could provide more insight into the abrupt change in volume observed in Figure 5.

Figure 6 shows the variation of the storage modulus and damping ($\tan \delta$) with temperature for dry-as-moulded and fully GW saturated PA66 samples. The $\tan \delta$ curves of the DaM sample exhibited two distinct peaks, labelled α and β , at about +71°C and -54°C respectively. It is well accepted that the α peak is associated with the motion of the longer chain segments in the amorphous sections of the polymer [26,32]. However, the β peak has been associated with both the presence of water and also with structural characteristics which are present in quenched samples but not in slow-cooled or annealed samples [32]. Since these samples had been stored in a desiccated atmosphere since moulding and the surface layers of injection moulded materials are most certainly quenched it might be concluded that the second of these two explanations may be correct in this case. However, it should also be noted that the bending mode of deformation used in this case would also preferentially probe the surface layer of the sample. Dry polyamides absorb moisture very rapidly in the surface layer and the exposure to a normal laboratory atmosphere during sample preparation, dimension

measurement and loading into the DMA instrument may have allowed enough moisture absorption into the sample to produce the β peak. The position of the α and β peaks for the DaM PA66 is well in line with the results of other published results [26,32,33] especially when taking into account that thermal analysis data on transition temperatures is always dependent on instrument, deformation mode, sample dimensions and thermal history and heating rate. The room temperature level of storage modulus for the DaM PA66 polymer (2.6 GPa) also agrees well with the value of Young's Modulus obtained on almost identical materials using standard tensile testing [3]. The curves in Figure 6 for the GW saturated polymer sample indicate the strong effect on the thermo-mechanical properties of PA66 caused by GW fluid absorption. Both α and β peaks are shifted to lower temperature, the α peak shows a greater shift of approximately 63°C to 8°C whereas the β peak shifts by only 6°C to -60°C. The storage modulus curves indicate a strong plasticisation of the polymer at room temperature. However there is an anti-plasticisation of the polymer at sub-ambient temperatures.

Figure 7 follows the evolution of the damping curve for PA66 polymer submerged in GW at 70°C with increasing time. It can be seen that 'shift' of the DaM α peak to lower temperature is not evidenced by a continuous shift in the peak temperature with increasing fluid uptake. The magnitude of the α peak at 71°C rapidly decreases with increasing exposure to hot GW and can no longer be resolved after 70 hours exposure. Simultaneously a damping peak (α^*) appears at approximately 10°C and grows in intensity with increasing fluid uptake. There is little evidence in Figure 7 of a shift in the α peak position to lower temperatures. Instead there appears to be a simultaneous decrease in the α peak height and an increase in the α^* peak height. There does not appear to be clear resolvable trend in the low temperature β peak in Figure 7. The trends

for the magnitude of the α and α^* peaks for the PA66 polymer are summarised in Figure 8. The data in Figure 8 clearly reveals the correlation between the reduction in the α peak and the increase in the α^* peak with the mass of absorbed fluid in the PA66 polymer. However this trend is not enough to fully explain the appearance of the α^* peak at 10°C which clearly indicates a separate underlying phenomenon related to the polymer fluid uptake.

Figure 9 follows the evolution of the storage modulus curve storage modulus for PA66 polymer submerged in GW at 70°C for increasing time. The principal observations in Figure 9 consist of a clear reduction of modulus in the 0-40°C temperature range with increasing fluid uptake. Simultaneously, an increase in the modulus in the sub-ambient temperature range is observed. The high temperature plasticisation of polyamides due to the ingress of moisture is well known [3,4,10-17,26,32]. Less well known is the low temperature increase in modulus. This has been attributed to the ability of water to form bonds between chain segments at low temperatures which are sufficiently stable to produce an increase in modulus [32]. The change in storage modulus at various temperatures compared to the weight of absorbed fluid in the PA66 polymer samples is presented in Figure 10. At -80°C there appears to be a significant increase in storage modulus with fluid content whereas at 25°C and 50°C there is an approximately linear decrease in the polymer modulus with the ingress of fluid. A further interesting observation in Figure 9 is the crossing of all the curves in the -10°C to 0°C temperature range. This is further highlighted in Figure 10 where it can be seen that the storage modulus at 0°C appears approximately independent of the polymer fluid uptake. At 80°C, above the DaM PA66 glass transition temperature, there is little evidence of a significant dependence of the storage modulus of fluid uptake. However, at this temperature (and higher) there must be considerable uncertainty in the actual fluid

content of the DMA sample which will be gradually drying out during the DMA measurement due to the elevated temperature.

Figures 11 and 12 present the summarised results for a similar analysis of the DMA performance of the series A composites. Figure 11, which shows the overview of the $\tan \delta$ peak analysis, reveals almost identical trends for the PA66 composite matrix as for the PA66 polymer results in Figure 8. It can be noted that the $\tan \delta$ level of the composite matrix material is significantly reduced by the presence of the glass fibre reinforcement. This phenomenon has been interpreted as an indication of the reduction of molecular mobility of the polymer molecules in the composite due to interaction with the fibre reinforcement [33]. As expected, the glass reinforcement also results in a significant increase in the modulus of the material across the whole temperature range of the measurements although it can be seen to have a proportionally larger effect at temperatures above the α transition which results in a 90% reduction in the stiffness of the polymer but only a 50% reduction in the stiffness of the composite.

As discussed above, typical testing for these composites in automotive applications involves measurement of mechanical properties before and after conditioning of the test material in model coolant fluids for a fixed time at temperatures in the 100-150°C range. In a previous report it was suggested that the results of mechanical property testing such as unnotched impact measured after different conditioning times and temperatures may be better understood when considered as a function of the level of fluid absorption and/or swelling obtained at any individual condition [17]. This possibility is examined further in Figures 13 and 14. These two figures present the mechanical performance of PA66 polymer and composites as a function of the level of fluid absorbed by the polymer (i.e. in the composites, the absorption level is normalised to the polymer

content). Data from this work obtained in GW mixtures at 70°C are compared with previously published [17] values obtained at 120°C and 150°C. The materials used in the previous report were based on the same grade of PA66, composite A* contained Owens Corning 123D chopped glass (a similar DaM optimized product) and composite B* contained Owens Corning 173X chopped glass (an older hydrolysis resistance optimized product). In Figure 13 the results for Young's modulus are presented, where the values have been normalised to the appropriate DaM value to eliminate small differences in testing conditions. The three groups of data in the Figure represent the different conditioning times at each temperature. It can be seen that there appears to be a good correlation between the trends observed in Young's modulus for both polymer and composite samples conditioned at three different temperatures when the data is considered in terms of the level of fluid uptake in the polymer (or composite matrix). The Young's modulus of these materials appears to decrease in a continuous manner with the increasing level of fluid uptake.

Figure 14 presents data for unnotched impact in a similar manner. Although the overall trend for unnotched impact is more complex than for Young's modulus it is clear that the data from the three conditioning temperatures do appear to fit well with each other. In particular the apparent peak in unnotched impact observed in the data from this work in Figure 3 is well confirmed when considered in reference to the results from higher temperature conditioning which appears to fit well with the reduction in impact observed as the level of fluid uptake is increased past the peak impact level of 7-8% fluid uptake. A further point to note in Figure 14 is the influence of the glass fibre sizing on the unnotched impact performance at different levels of fluid uptake. At short conditioning times (and/or low conditioning temperatures) the normalised data for composites A and B show little significant difference in relative performance. The

influence of the hydrolysis resistance optimised sizing only begins to become apparent at conditions which result in a fluid uptake of greater than 5% weight. This difference appears to become greater in the range 5-20% fluid uptake. However, under extreme conditioning (longer times at high temperatures) the influence of the fibre sizing is reduced as the unnotched impact of all composites falls to a very low level. Overall, these results would seem to offer the possibility of predicting performance at any conditioning time and temperature from data obtained under different conditions. This is an area which requires further investigation.

Conclusions

This study of injection moulded glass-fibre reinforced polyamide 66 composites has revealed that hydrothermal conditioning in water-glycol mixtures results in significant changes in the weight, dimensions, and thermo-mechanical performance of these materials. All materials showed a weight increase due to hydrothermal conditioning at 70°C which was typical of a pseudo-Fickian diffusion process. It was noted that the presence of the glass fibres reduced the fluid uptake by an amount significantly greater than would be expected from a simple scaling with the polymer content of the composites. DMA analysis indicated a large reduction in glass transition temperature of the PA66 after saturation in glycol-water mixtures. However, further investigation revealed that this was not due to a continuous downward shift in the $\tan \delta$ α peak, but due to the simultaneous decrease in the high temperature α damping peak and appearance and growth of a low temperature α^* damping peak. Glycol-water absorption caused a significant reduction in the DMA storage modulus in the 0-40°C range. However, the sub-ambient storage modulus was significantly increased by fluid absorption. The modulus of the conditioned polymer and composite samples decreased continuously with increasing condition time and fluid absorption levels. The unnotched Charpy impact performance exhibited more complicated trends. Initially the impact strength fell with increasing conditioning time but after approximately 25 hours went through a sharp rise reaching a maximum level approximately 40% above the DaM values. Further increase in conditioning time was followed by a gradual decrease in impact performance. When compared to mechanical performance after conditioning at higher temperatures these data appeared to form continuous performance curves when considered as a function of the level of adsorbed fluid in the composite matrix. The results on dimensional change and unnotched impact indicated the presence of an abrupt

change in the structure-performance relationship of PA66 after absorbing 5-6% wt. glycol-water mixture at 70°C.

Acknowledgement

The author gratefully acknowledges the support of 3B Fibreglass, Battice, Belgium with the preparation and moulding of the materials used in this study.

References

1. Sato N, Kurauchi T, Sato S, and Kamigaito O. Reinforcing mechanism by small diameter fiber in short fiber composites. *J. Compos. Mater.* 1998;22:850-873
2. Hassan A, Yahya R, Yahaya AH, Tahir ARM, Hornsby PR. Tensile, Impact and Fiber Length Properties of Injection-molded Short and Long Glass Fiber-reinforced Polyamide 6,6 Composites. *J.Reinforced Plastics and Composites* 2004;23:969-986.
3. Thomason JL. Structure-property relationships in glass reinforced polyamide: 1) The effect of fibre content. *Polym.Composites* 2006;27:552-562.
4. Thomason JL. Structure-property relationships in glass reinforced polyamide: 2) The effects of average fibre diameter and diameter distribution. *Polym.Composites* 2007;27:331-343.
5. Mouhmid B, Imad A, Benseddiq N, Benmedakhène S, Maazouz A. A study of the mechanical behaviour of a glass fibre reinforced polyamide 6,6. *Polymer Testing* 2006;25:544-552.
6. Carlson E, Nelson K. Nylon under the hood: history of innovation. *Automotive Engineering* 1996;104:84-89.
7. Harrison AR. Automotive Composite Components, Chapter 11 in *Integrated Design and Manufacture Using Fibre-reinforced Polymeric Composites*. Eds. Owen MJ. Middleton V. Woodhead Publishing, 2000.
8. Rudd CD. Composites for Automotive Applications, *Rapra Review Reports Volume 11, number 6, 2000, page 12*. Published by iSmithers Rapra, 2001
9. Page IB. Polyamides As Engineering Thermoplastic Materials. *Rapra Review Reports Volume 11, number 1, 2000, page 13*. Published by iSmithers Rapra, 2001.

10. Gavenonis J, McIlvaine JE. Polyamide Resin Technologies for High Temperature and Automotive Chemical Exposure Environments, Society of Automotive Engineers Technical Paper Series, 2009, 2009-01-1297.
11. Valentin D, Paray F, Guetta B. The Hygrothermal Behaviour of Glass Fibre Reinforced Pa66: a study of the effect of water absorption on their mechanical properties. *J.Mater.Sci.* 1987;22:46-56.
12. Mohd Ishak ZA, Berry JP. Hygrothermal Aging Studies of Short Carbon Fiber Reinforced Nylon 6.6. *J.Appl.Polym.Sci.* 1991;54:2145-2155.
13. Takeda N, Song D, Nakata K. Effects of temperature and water content on impact properties on injection-molded glass nylon-6 composites . *Adv. Composite Mater.* 1996;5:201-212.
14. Bergeret A, Pires I, Foulc MP, Abadie B, Ferry L, Crespy A. The hygrothermal behaviour of glass fibre reinforced thermoplastic composites. *Polym Testing* 2001;20:753-763.
15. Jia N, Fraenkel HA, Kagan VA. Effects of moisture conditioning methods on mechanical properties of injection molded nylon 6. *J.Reinforced Plastics and Composites* 2004;23:729-737.
16. I. Carrascal, J.A. Casado, J.A. Polanco, F. Gutiérrez-Solana, Absorption and diffusion of humidity in fiberglass-reinforced polyamide. *Polymer Composites* 2005;26:580-586.
17. Thomason JL. Structure-property relationships in glass reinforced polyamide: 3) Effects of hydrolysis ageing on the dimensional stability and performance of short glass-fibre reinforced Polyamide 66. *Polym.Composites* 2007;27:344-354.
18. Thomason JL and Ali JZ. The dimensional stability of glass-fibre reinforced Polyamide 66 during hydrolysis conditioning. *Composites Part A* 2009;40:623-634.

19. Coakley TA, Rubadue JE, Forman CE, Schweizer RA. Non-discoloring glass strand size. United States Patent 4,255,317 (1981)
20. Thomason JL, Adzima LJ. Sizing up the interface: an insider's guide to the science of science. *Composites Part A* 2001;32:313-321.
21. Cossement M, Masson N, Piret W. Size composition. United States Patent 5,236,982 (1993)
22. Masson N, Henrion JM, Thomason JL, Adzima LJ, Cheney TL, Piret W, Cossement M. System for preparing glass fiber pellets having low discoloration. United States Patent 6,365,272 (2002)
23. Cossement M, Henrion JM. Two-part sizing composition for reinforcement fibers Patent United States Patent Application 20070154697 (2007)
24. Crank J, Park GS. (eds) *Diffusion in Polymers*, Academic Press, New York, 1968
25. Starink MJ, Starink LMP, Chambers AR. Moisture uptake in monolithic and composite materials: edge correction for rectangularoid samples. *J.Mater.Sci.* 2002;37:287-294.
26. Valle´S-Lluch A, Camacho W, Ribes-Greus A, Karlsson S. Influence of Water on the Viscoelastic Behavior of Recycled Nylon 6,6. *J.Appl.Polym.Sci.* 2002;85: 2211–2218.
27. Brill R. *J Prakt Chem* 1942;161;49-64.
28. Murthy NS, Curran SA, Aharoni SM and Minor H. Premelting Crystalline Relaxations and Phase Transitions in Nylon 6 and 6,6. *Macromolecules* 1991;24:3215-3220.
29. Xenopoulos A and Clark ES. Chapter 5 Nylon plastics handbook, Kohan MI, Editor Hanser Gardener, Cincinnati (1995).
30. Starkweather HW and Jones GA. Crystalline transitions in powders of nylon 66 crystallized from solution. *J.Polym.Sci. Polym.Phys.Ed.* 81;19:467

31. Murthy NS, Akkapeddi MK, and Orts W. Analysis of Lamellar Structure in Semicrystalline Polymers by Studying the Absorption of Water and Ethylene Glycol in Nylons Using Small-Angle Neutron Scattering. *Macromolecules* 1998;1:142-152
32. Starkweather HW. Chapter 6 Nylon plastics handbook, Kohan MI, Editor Hanser Gardener, Cincinnati (1995).
33. Klein N, Marom G, Pegoretti A and Migliaresi C. Determining the role of interfacial transcrystallinity in composite materials by dynamic mechanical thermal analysis. *Composites* 1995;26:707-712.

List of Figures

Figure 1 Weight gain of polymer, composites, and composite matrix versus conditioning time at 70°C

Figure 2 Fitting of time dependent diffusion coefficient to weight gain data

Figure 3 Unnotched Charpy impact versus conditioning time at 70°C

Figure 4 Unnotched Charpy impact versus polymer/matrix weight increase

Figure 5 Volume change versus weight increase

Figure 6 DMA analysis DaM and GW saturated PA66

Figure 7 DMA $\tan \delta$ curves for PA66 at different GW conditioning times

Figure 8 DMA $\tan \delta$ trends for conditioned PA66

Figure 9 DMA storage modulus curves for PA66 at different GW conditioning times

Figure 10 DMA storage modulus trends for GW conditioned PA66

Figure 11 DMA $\tan \delta$ trends for conditioned GFPA66

Figure 12 DMA storage modulus trends for GW conditioned GFPA66

Figure 13 Relative modulus versus GW fluid absorption at different temperatures

Figure 14 Relative unnotched impact versus GW fluid absorption at different temperatures

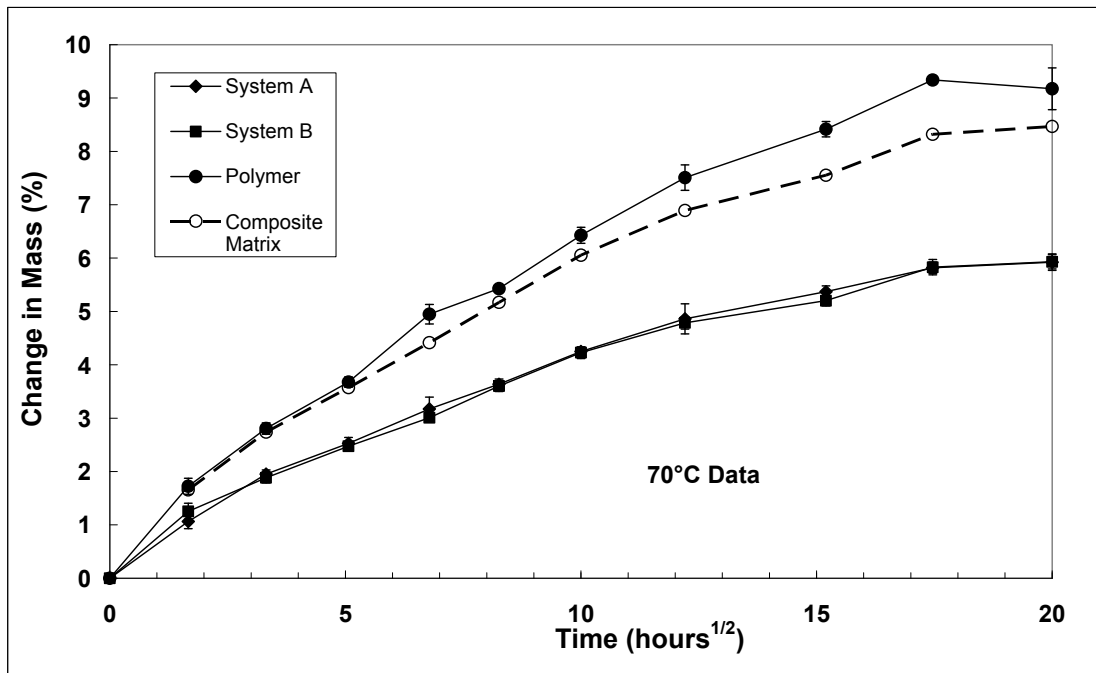


Figure 1 Weight gain of polymer, composites, and composite matrix versus conditioning time at 70°C

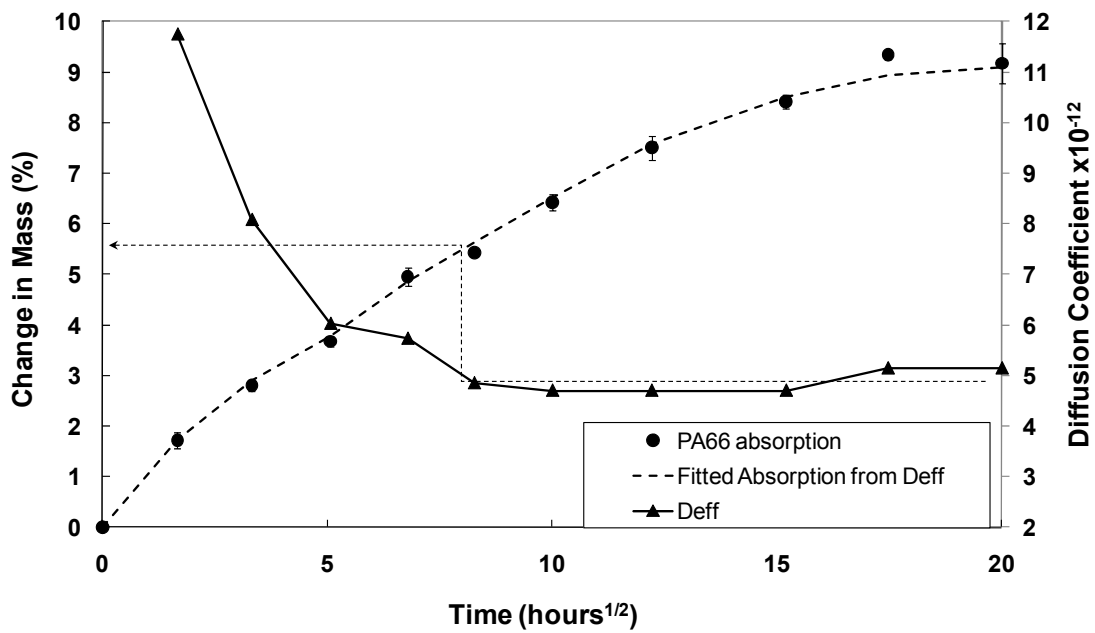


Figure 2 Fitting of time dependent diffusion coefficient to weight gain data

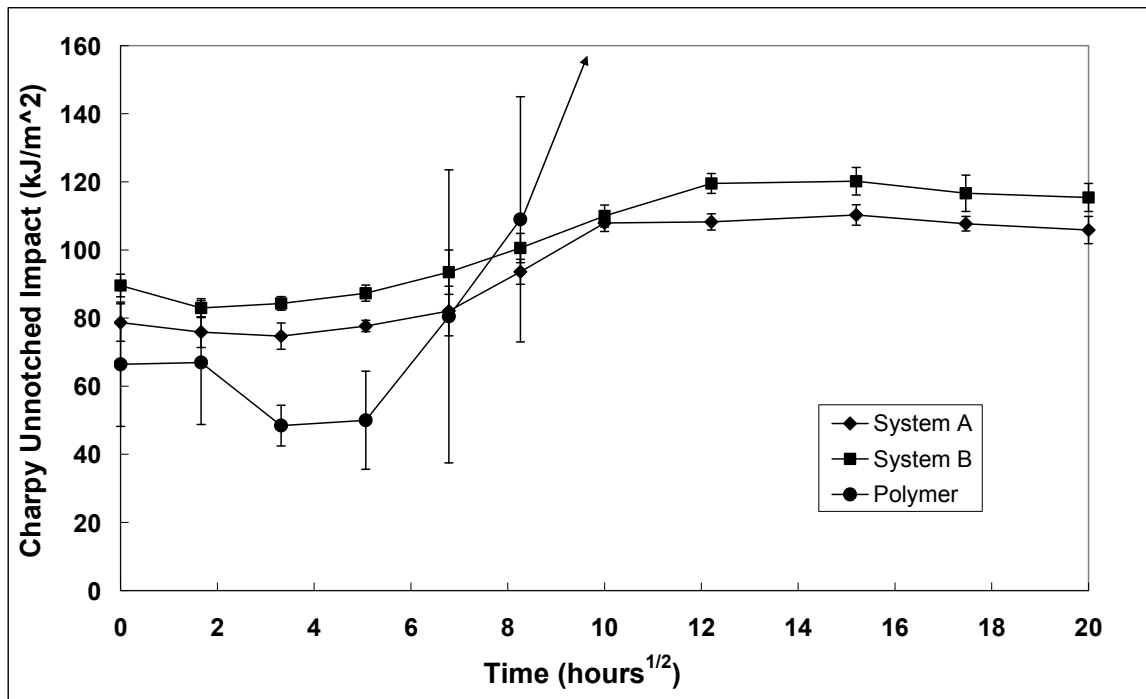


Figure 3 Unnotched Charpy impact versus conditioning time at 70°C

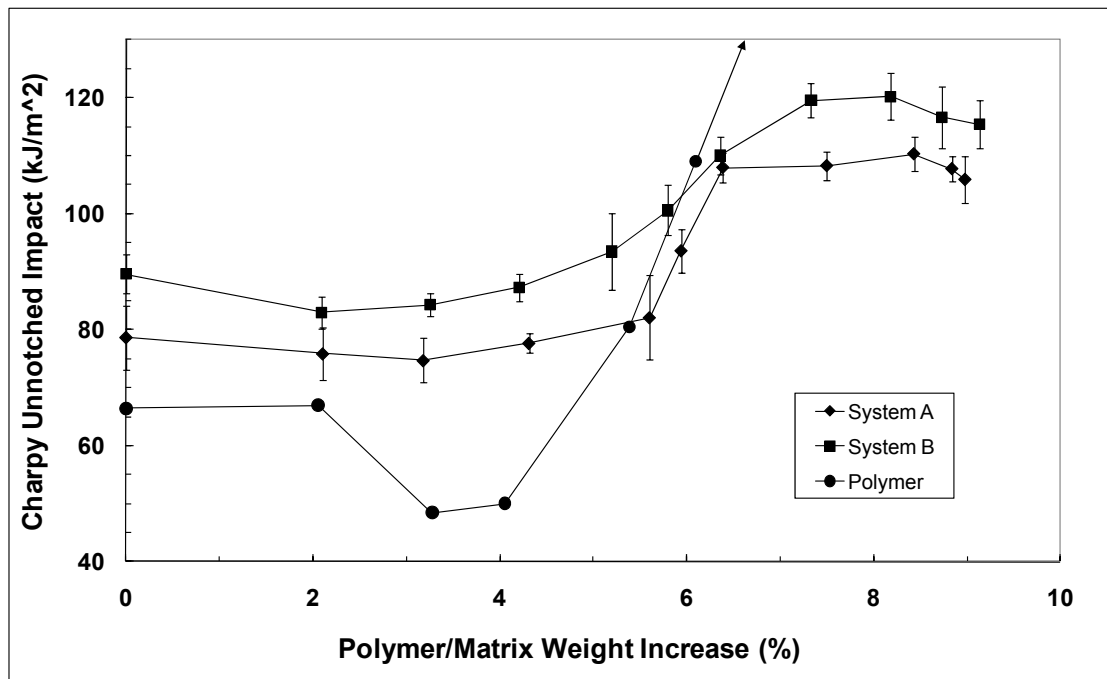


Figure 4 Unnotched Charpy impact versus polymer/matrix weight increase

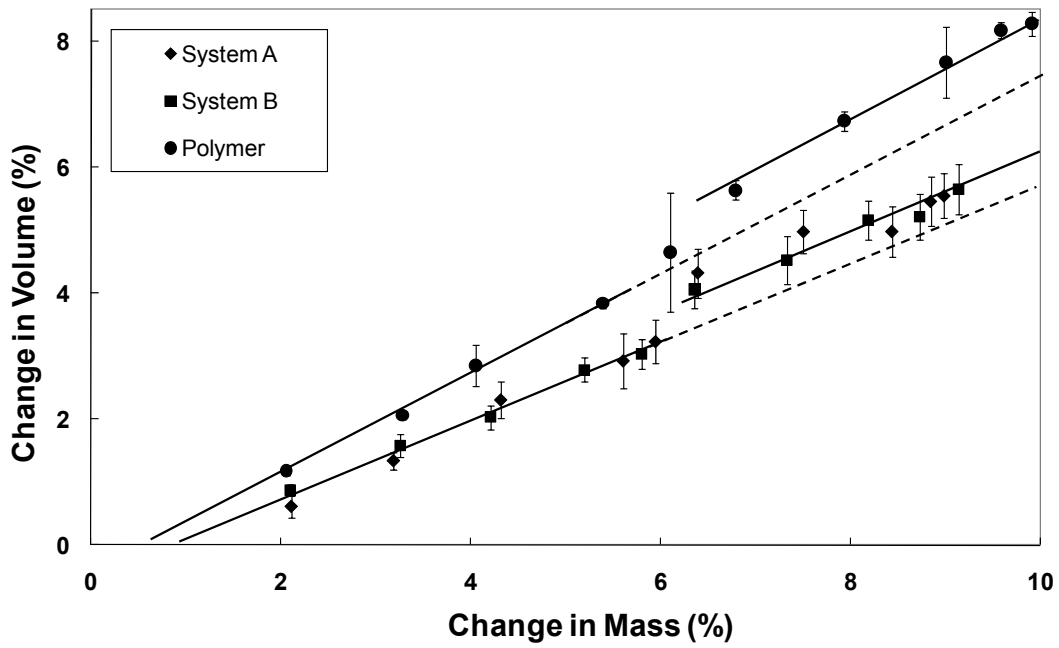


Figure 5 Volume change versus weight increase

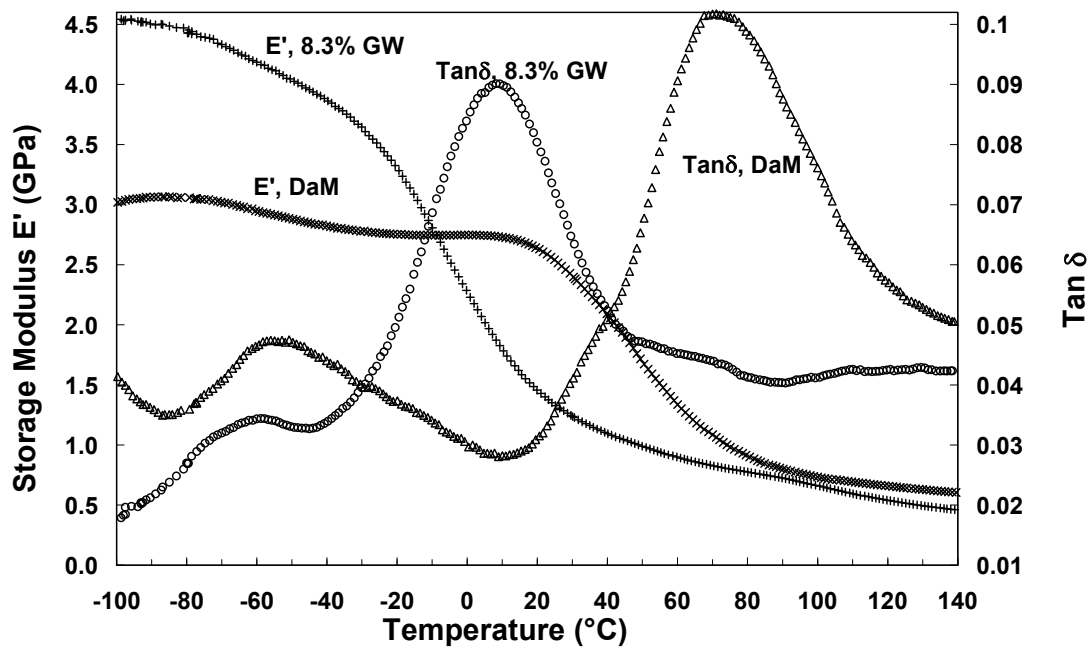


Figure 6 DMA analysis DaM and GW saturated PA66

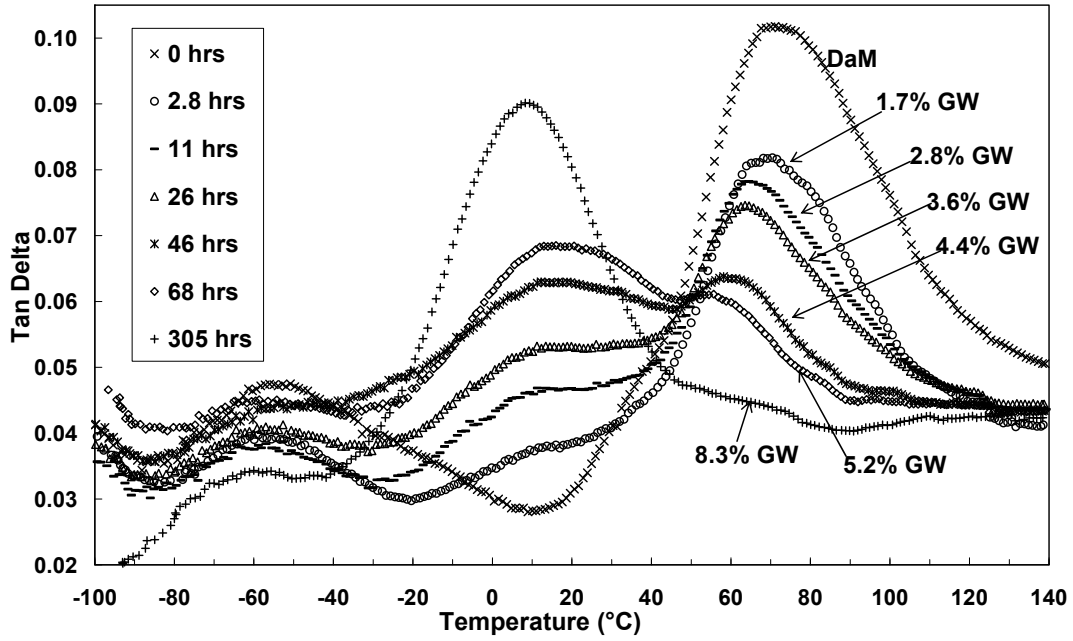


Figure 7 DMA tan δ curves for PA66 at different GW conditioning times

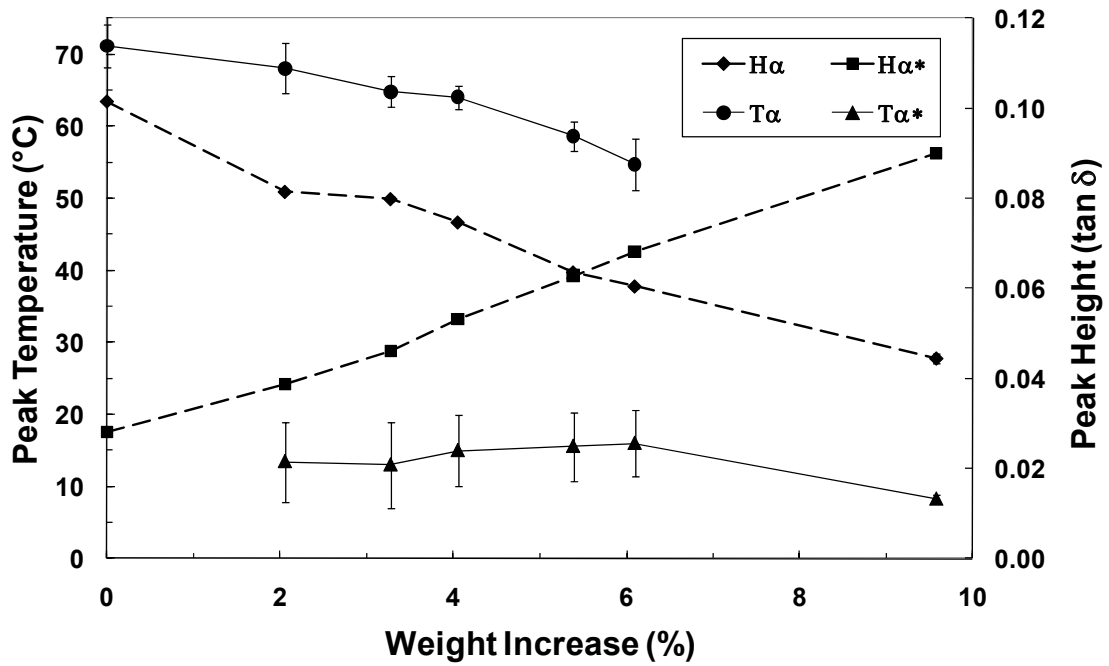


Figure 8 DMA Tan δ trends for GW conditioned PA66

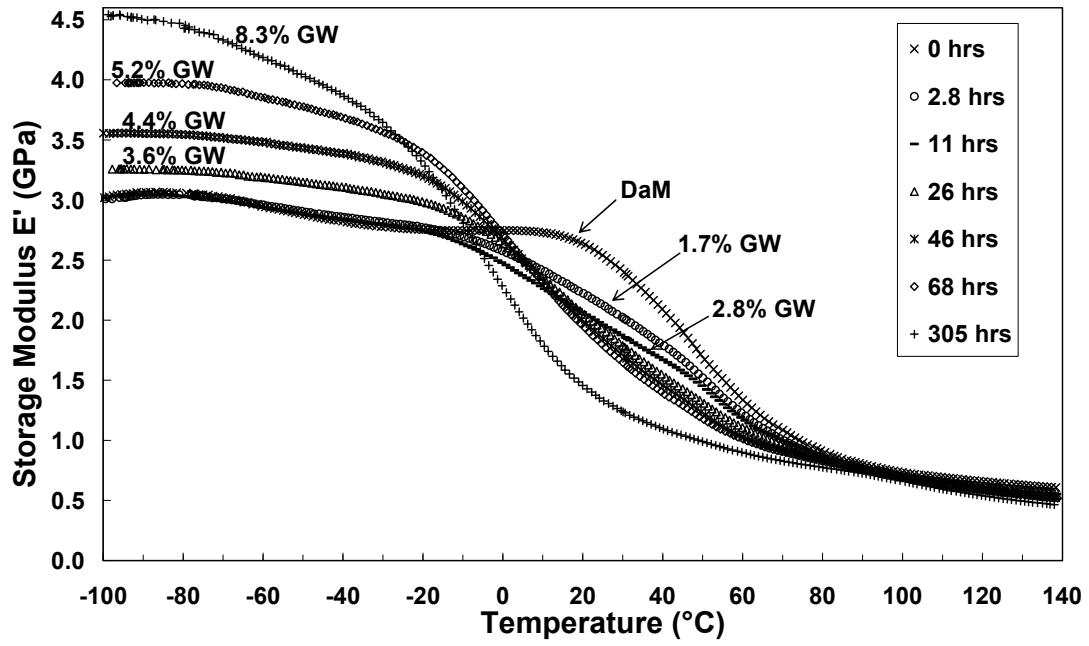


Figure 9 DMA storage modulus curves for PA66 at different GW conditioning times

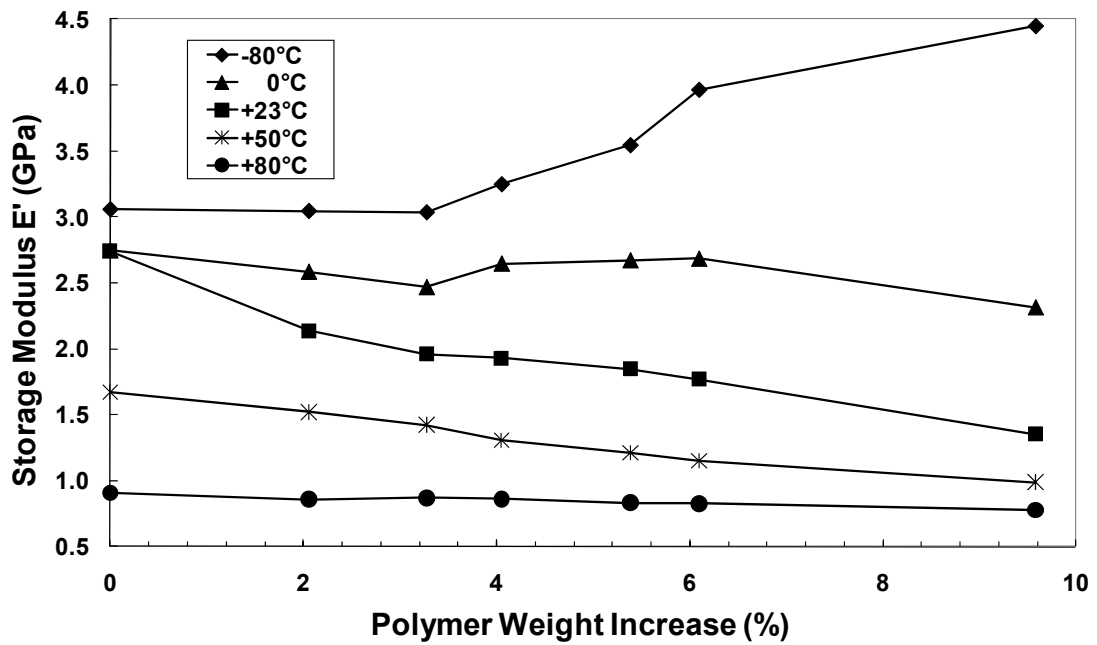


Figure 10 DMA storage modulus trends for GW conditioned PA66

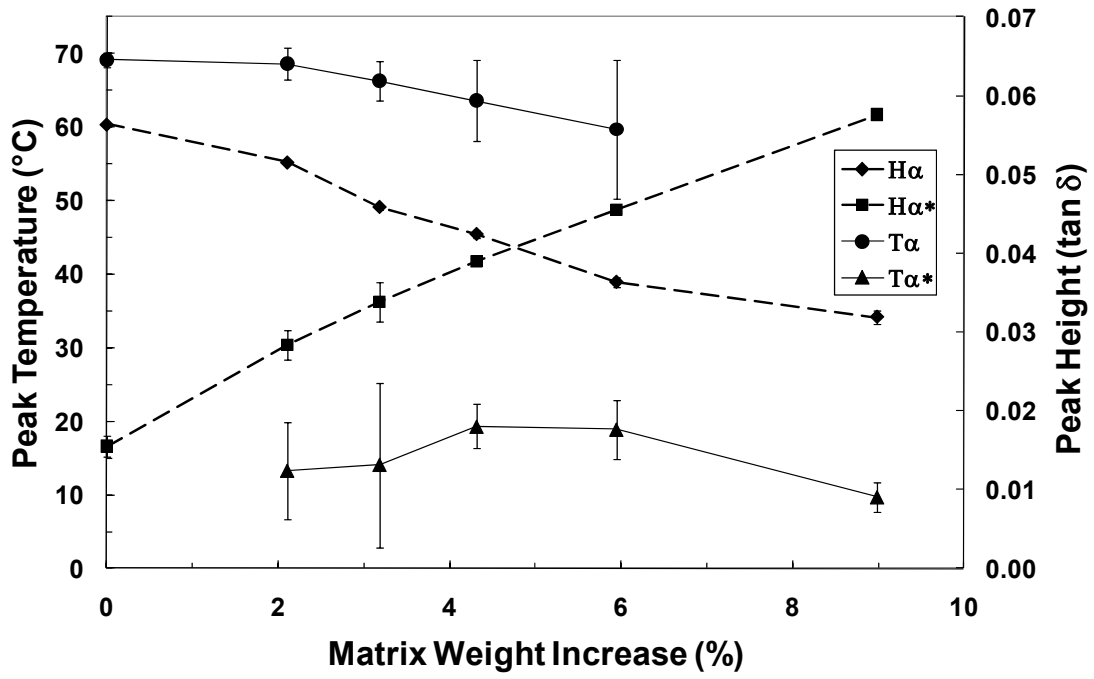


Figure 11 DMA Tan δ trends for conditioned GFPA66

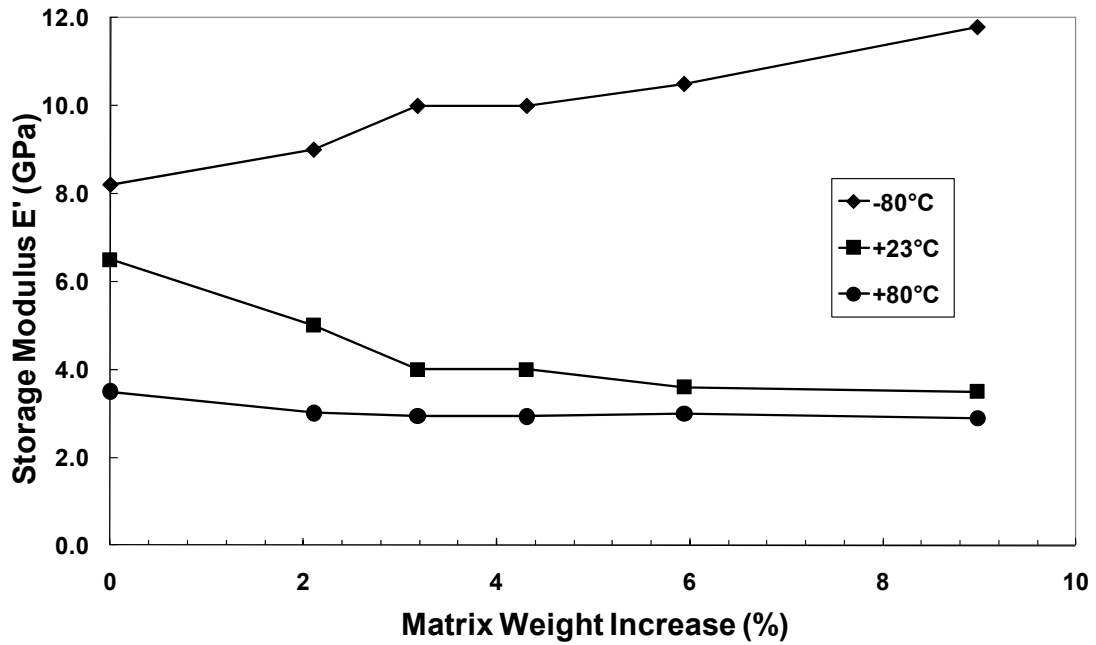


Figure 12 DMA storage modulus trends for GW conditioned GFPA66

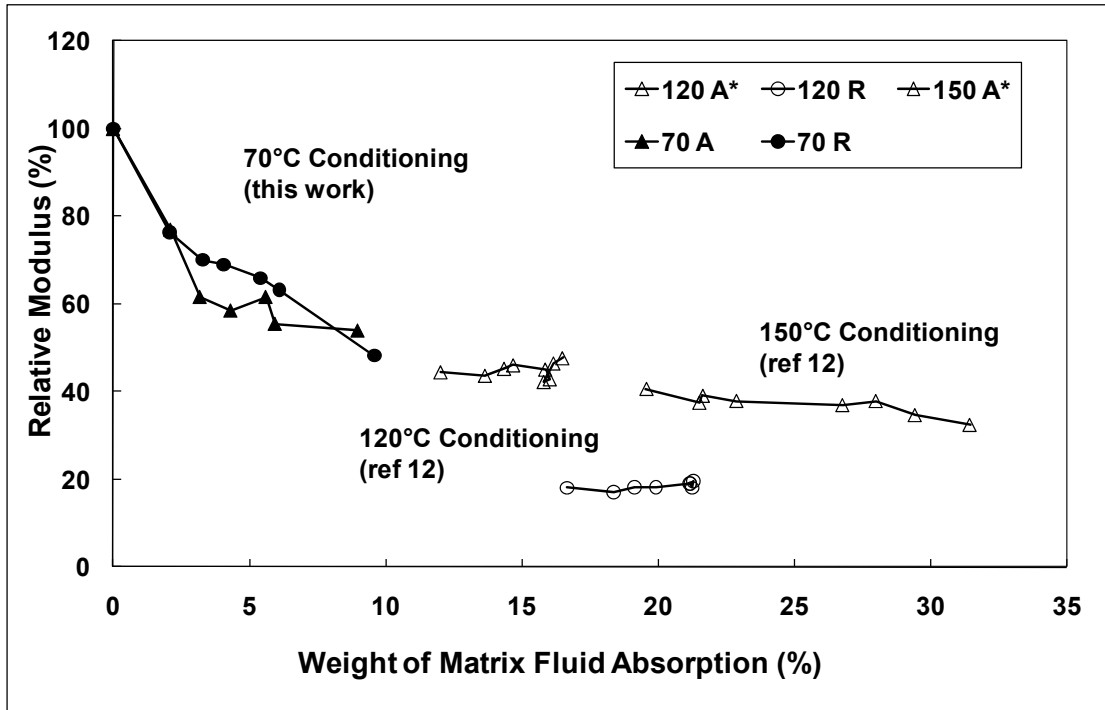


Figure 13 Relative modulus versus GW fluid absorption at different temperatures

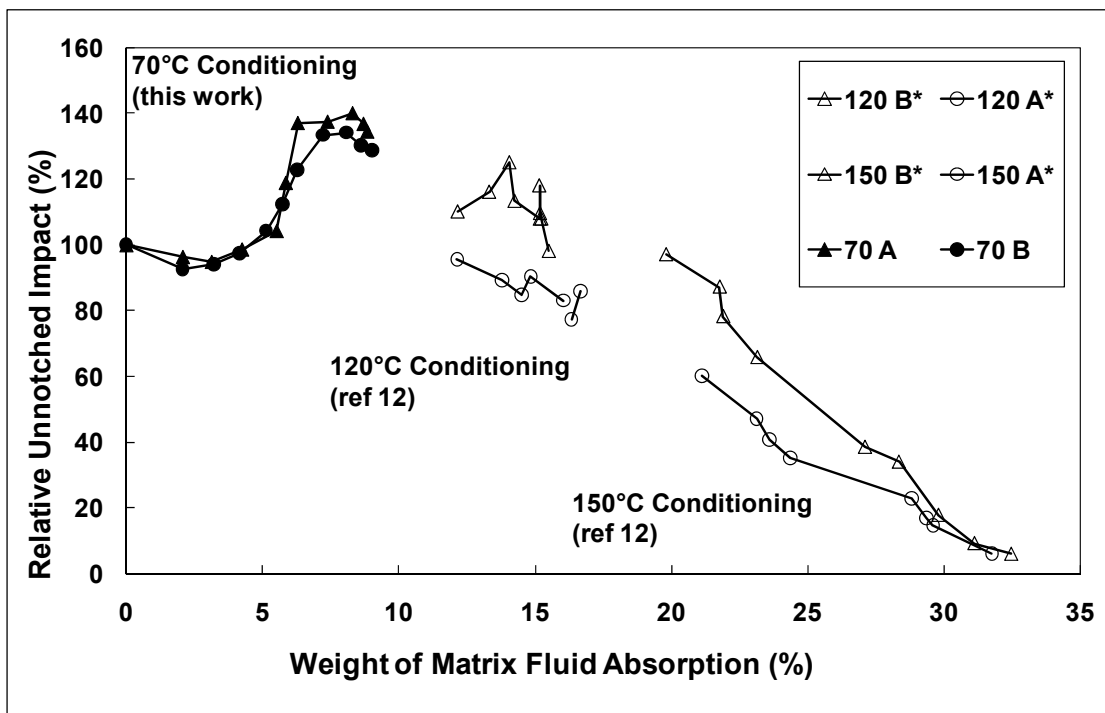


Figure 14 Relative unnotched impact versus GW fluid absorption at different temperatures